LETTER

Cluster preformation at the nuclear surface in cold fission

To cite this article: D. N. Poenaru and R. A. Gherghescu 2017 *EPL* **118** 22001

A Letters Journal Exploring the Frontiers of Physics

April 2017

EPL, **118** (2017) 22001 www.epljournal.org
doi: 10.1209/0295-5075/118/22001

Cluster preformation at the nuclear surface in cold fission

D. N. Poenaru and R. A. Gherghescu

Horia Hulubei National Institute of Physics and Nuclear Engineering (IFIN-HH) - P.O. Box MG-6, RO-077125 Bucharest-Magurele, Romania and
Frankfurt Institute for Advanced Studies, Johann Wolfgang Goethe University - Ruth-Moufang-Str. 1, D-60438 Frankfurt am Main, Germany

received 28 January 2017; accepted in final form 8 June 2017
published online 26 June 2017

PACS 25.85.Ca – Spontaneous fission
PACS 24.75.+i – General properties of fission
PACS 21.60.Cs – Shell model

Abstract – Microscopic theories of alpha decay and cluster radioactivity explain these decay modes as a quantum tunnelling of a preformed cluster at the nuclear surface. In the present work we show that in a spontaneous cold-fission process the shell plus pairing corrections, calculated with Strutinsky's procedure based on the two-center shell model, may give a strong argument for preformation of a light fission fragment near the nuclear surface. It is obtained when the radius of the light fragment, R_2, is increased linearly with the separation distance, R, of the two fragments, while for $R_2 = \text{const}$ one gets the well-known two-hump potential barrier for heavy and superheavy nuclei. Nuclear-physics community also contributed to nanocluster physics by applying the macroscopic-microscopic method to explain the shell effects experimentally observed since 1984. Applications are shown for two nuclei, ^{260}Rf and ^{264}Sg, whose half-life against spontaneous fission is very well known. We stress a new aspect of the cold spontaneous fission, unifying its theory with that of α- and cluster decays, all having in common a preformed light cluster which will penetrate the potential barrier by quantum tunelling.

Introduction. – In 1928 Gamow [1] as well as Condon and Gurney [2] gave the first explanation of alpha decay as a quantum tunnelling of a preformed particle at the nuclear surface. It was the first application of quantum mechanics to nuclear physics. Soon after the experimental discovery in 1984 by Rose and Jones [3] of cluster radioactivity, confirming the earlier (1980) predictions [4], a microscopic theory [5] also explained the phenomenon in a similar way. After 1928 the microscopic theories of α-decay have been developed, see, *e.g.*, [6]. Simple relationships are also very useful [7,8] to estimate the half-lives.

Spontaneous fission was discovered in 1940 by Flerov and Petrzhak. Usually the fission fragments are deformed and excited; they decay by neutron emission and/or γ-rays, so that the total kinetic energy (TKE) of the fragments is smaller by about 25–35 MeV than the released energy, or Q-value. The asymmetric mass distributions of the fission fragments and the spontaneously fissioning shape isomers [9] could not be explained until 1967, when Strutinsky reported [10] his macroscopic-microscopic method. His calculations gave for the first time a two-hump potential barrier. Shape isomers occupied the second minimum. A brief presentation, at a level of non-specialist, of the large diversity of nuclear decay modes may be found in ref. [11].

Superheavy nuclei with atomic numbers $Z = 104$–118 are produced by fusion reactions [12,13]. The simplest way to identify a new superheavy element synthesized in such a way is to measure its α-decay chain, down to a known nuclide. Sometimes this is not possible since its main decay mode could be spontaneous fission. For atomic numbers larger than 121 cluster decay may compete as well [14]. Among the many theoretical papers in this field one should mention [15–17].

It is also important to mention the contribution of nuclear physicists, *e.g.*, [18,19], who adapted the nuclear macroscopic-microscopic theory to atomic cluster physics, where the shell effects have been observed since 1984 [20].

We reported [21,22] results obtained within the macroscopic-microscopic method using cranking inertia [23] and the best two-center shell model [24] in the space of two independent variables (R, η), where R is the separation distance of the fragments and $\eta = (A_1 - A_2)/A$

is the mass asymmetry with A, A_1, A_2 the mass numbers of the parent and nuclear fragments. Phenomenological deformation energy, E_{Y+E}, was given by the Yukawa-plus-exponential model [25], and the shell plus pairing corrections, $\delta E = \delta U + \delta P$ are based on the asymmetric two-center shell model (ATCSM). This time we give more detailed arguments for two superheavies (SHs) with well-known spontaneous fission (SF) half-lives: ^{260}Rf and ^{264}Sg. The deep minimum of total deformation energy near the surface is shown as a strong argument for light fragment preformation in cold fission, discovered in 1981 [26]. It is obtained when the radius of the light fragment, R_2, is increased linearly with the separation distance, R, of the two fragments, while for $R_2 = \text{const}$ one gets the well-known two-hump potential barrier.

While usually the disagreement of calculated spontaneous fission half-lives, even with the most advanced models like density functional theory [16] or Hartree-Fock-Bogoliubov approach with the finite-range and density-dependent Gogny force with the D1S parameter set [17] may be as high as ten orders of magnitude, we succeeded with our method to get values under one order of magnitude —looking very promising. Our work gives an interesting new aspect of the cold spontaneous fission, unifying its theory with that of α- and cluster decays, all having in common a preformed light cluster which will penetrate the potential barrier by quantum tunnelling.

Results. – An outline of the model was presented previously [21]. Here we repeat just few lines. The parent ^{A}Z is split in two fragments: the light, $^{A_2}Z_2$, and the heavy one, $^{A_1}Z_1$, with conservation of hadron numbers $A = A_1 + A_2$ and $Z = Z_1 + Z_2$. The corresponding radii are given by $R_0 = r_0 A^{1/3}$, $R_{2f} = r_0 A_2^{1/3}$, and $R_{1f} = r_0 A_1^{1/3}$ with $r_0 = 1.16\,\text{fm}$. The separation distance of the fragments is initially $R_i = R_0$ and at the touching point it is $R_t = R_{1f} + R_{2f}$. The geometry for linearly increasing R_2 from 0 to $R_{2f} = R_e$ is defined by

$$R_2 = R_{2f} \frac{R - R_i}{R_t - R_i}. \tag{1}$$

We consider only spherical shapes allowing to have only two shape independent coordinates: the separation distance, R, and the mass asymmetry parameter $\eta = (A_1 - A_2)/A$. An example of the shape evolution, corresponding to the above equation and to $R_2 = \text{const}$ is given in fig. 1 for symmetrical fission of ^{264}Sg. There are 6 stages for $x = 0, 0.2, 0.4, 0.6, 0.8$ and 1, meaning from a parent nucleus, $x = 0$, to the touching point of the two fragments, $x = 1$. The pear-shapes in the early stages are clearly witnessing the octupole deformation, but near the scission one has again reflexion symmetric shapes. This transition leads to higher fission barriers. Two examples of microscopic calculations may be seen in refs. [27,28].

According to the macroscopic-microscopic method the total deformation energy contains the macroscopic Yukawa-plus-exponential (Y+EM) term and the shell plus pairing corrections,

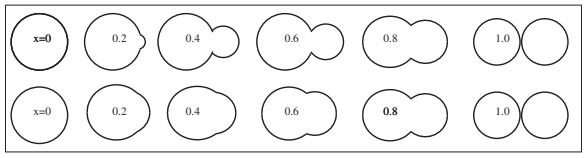

Fig. 1: Shape evolutions during the symmetrical spontaneous fission of ^{264}Sg from one parent nucleus, to two touching fragments *vs.* $x = (R - R_i)/(R_t - R_i)$ when the radius R_2 of the light fragment is linearly increasing (top) and $R_2 = \text{const}$ (bottom).

$$E_{def} = E_{Y+E} + \delta E. \tag{2}$$

In units of $\hbar\omega_0^0 = 41 A^{-1/3}$ the shell corrections are calculated with the Strutinsky procedure as a sum of protons and neutrons contributions,

$$\delta u = \delta u_p + \delta u_n. \tag{3}$$

One obtains a minimum when there are important bunchings of levels (high degeneracy of the quantum state: the same energy corresponds to several states).

The BCS [29] theory was first introduced in condensed matter in order to explain the superconductivity at a very low temperature. It was extended to nuclei for the explanation of the pairing interaction, see, *e.g.*, [23].

For pairing corrections we have first to solve the BCS [29] system of two equations with two unknowns, Fermi energy λ and the pairing gap Δ,

$$0 = \sum_{k_i}^{k_f} \frac{\epsilon_k - \lambda}{\sqrt{(\epsilon_k - \lambda)^2 + \Delta^2}}, \tag{4}$$

$$\frac{2}{G} = \sum_{k_i}^{k_f} \frac{1}{\sqrt{(\epsilon_k - \lambda)^2 + \Delta^2}}, \tag{5}$$

where $k_i = Z/2 - n + 1, k_f = Z/2 + n'$ for proton levels. We use $G = \text{const}$, and the energy window corresponds to about one shell, enough to make any further contribution of other levels negligibly small.

Finally the total shell plus pairing corrections in MeV are

$$\delta E = \delta U + \delta P. \tag{6}$$

Pairing correction is in general smaller in amplitude and in antiphase with shell correction; it has an effect of smoothing and reducing the total shell plus pairing correction energy. The experience of using Strutinsky's method, gained by several nuclear scientists (*e.g.*, S. Bjørnholm), was also successfully employed to study shell effects in atomic cluster physics and nanotechnology.

In fig. 2 we present the contour plot of the macroscopic (Y+EM) deformation energy for ^{264}Sg with two fission paths corresponding to $R_2 = \text{const}$ and R_2 linearly increasing. One can see how complicated can be the path

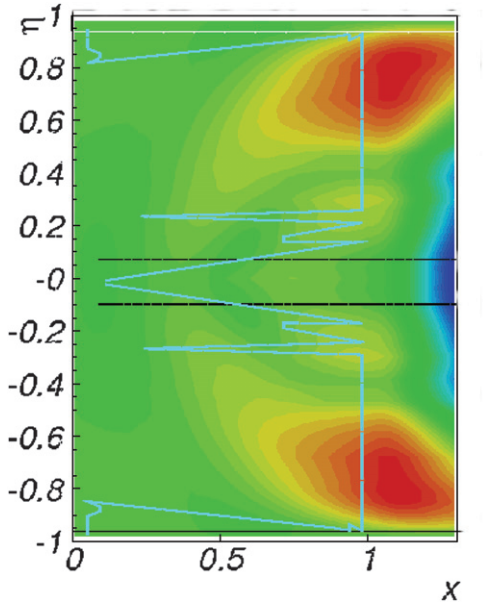

Fig. 2: (Colour online) Contour plot of macroscopic (Y+EM) deformation energy for symmetrical spontaneous fission of ^{264}Sg *vs.* separation $x = (R-R_i)/(R_t-R_i)$ and mass asymmetry $\eta = (A_1 - A_2)/A$. Two fission paths are shown: for linearly increasing R_2 with continuous line and for R_2 = const with dashed line. The deformation energy scale: from a minimum of -42 MeV to a maximum of 28 MeV.

for linearly increasing R_2, compared to the simple one for R_2 = const. What is missing is the exit from the barrier for linearly increasing R_2; one should take it at the small asymmetry near $\eta = 0.1$. The least action trajectory, determined by our computer program, goes through the minima of the action integral, which depends on the product of total deformation energy and the cranking inertia, and the jumps shown by the cyan line are determined by this rule.

We can understand better the reality by looking at fig. 3 in which the total deformation energy (at the top) and the cranking inertia (at the bottom) along this path are shown. The product of these two quantities is determining the half-life as shown in eq. (10). While the inertia is very large at small x, the deformation energy is small there; its highest peak stands around $R = 10$, where the inertia is already equal to the reduced mass, as it should be at the touching point. By multiplying cranking inertia by total deformation energy, which is quite small there, and then taking the square root in a narrow interval of R, as may be seen from fig. 3, the total effect on the half-life is not very big.

Any component of the inertia tensor [23] is given by

$$B_{ij} = 2\hbar^2 \sum_{\nu\mu} \frac{\langle\nu|\partial H/\partial\beta_i|\mu\rangle\langle\mu|\partial H/\partial\beta_j|\nu\rangle}{(E_\nu + E_\mu)^3}(u_\nu v_\mu + u_\mu v_\nu)^2, \tag{7}$$

where H is the single-particle Hamiltonian allowing to determine the energy levels and the wave functions $|\nu\rangle$;

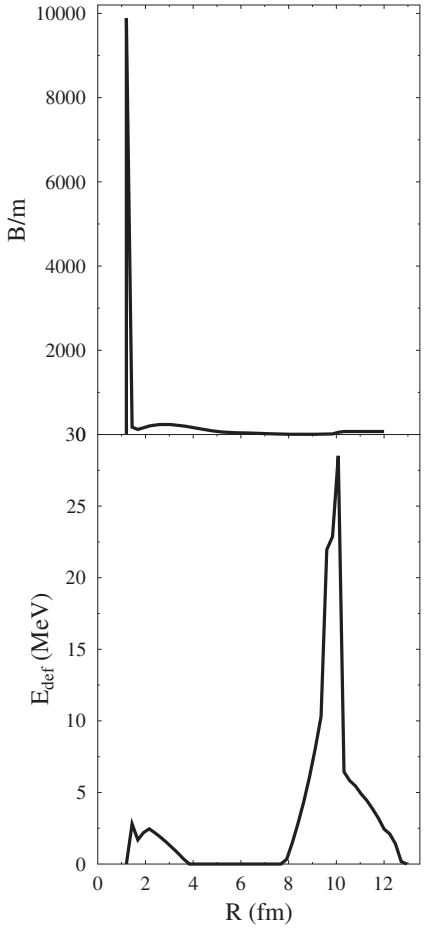

Fig. 3: Total deformation energy and cranking inertia for ^{264}Sg symmetrical spontaneous fission *vs.* separation distance R along the fission path for linearly increasing R_2 shown in fig. 2. m is the nucleon mass.

u_ν^2, v_ν^2 are the BCS occupation probabilities, E_ν is the quasiparticle energy, and β_i, β_j are the independent shape coordinates.

For spherical fragments with R, R_2 deformation parameters, the cranking inertia symmetrical tensor will have three components, hence the scalar

$$B(R) = B_{R_2R_2}\left(\frac{\mathrm{d}R_2}{\mathrm{d}R}\right)^2 + 2B_{R_2R}\frac{\mathrm{d}R_2}{\mathrm{d}R} + B_{RR} \tag{8}$$

or $B = B_{22} + B_{21} + B_{11}$. When we find the least action trajectory in the plane (R, R_2), we need to calculate the three components B_{22}, B_{21}, B_{11} in every point of a grid of 66×24 (for graphics) or 412×24 (for the real calculation) for 66 or 412 values of $(R - R_i)/(R_t - R_i)$ and 24 values of $\eta = (A_1 - A_2)/A$ or R_{2f}.

The half-life of a parent nucleus against spontaneous fission is given by

$$T = [(h \ln 2)/(2E_v)]exp(K_{ov} + K_s) \tag{9}$$

and is calculated by using the Wentzel-Kramers-Brillouin (WKB) quasiclassical approximation, according to which

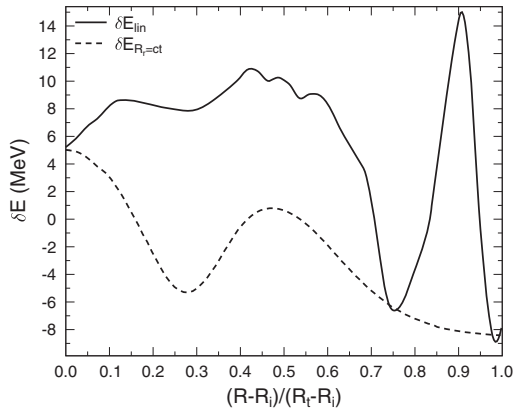

Fig. 4: Comparison of absolute values of shell and pairing correction energies for symmetrical fission of ^{260}Rf with R_2 constant (dashed line) and linearly increasing R_2 (solid line).

the action integral is expressed as

$$K = \frac{2\sqrt{2m}}{\hbar} \int_{R_a}^{R_b} \{[(B(R)/m)][E_{def}(R) - E_{def}(R_a)]\}^{1/2} \mathrm{d}R \tag{10}$$

with m the nucleon mass, $B =$ the cranking inertia (see the equation above), $K = K_{ov} + K_s$, and the $E(R) = E_{def}$ potential energy of deformation. R_a and R_b are the turning points of the WKB integral where $E_{def} = E_{def}(R_a) = E_{def}(R_b)$. The two terms of the action integral K, correspond to the overlapping (K_{ov}) and separated (K_s) fragments.

In order to illustrate the basic idea of this work, namely there is a minimum of the total deformation energy, E_{def}, near the surface, produced both by microscopic shell and pairing corrections, δE (fig. 4 and fig. 5 at the top), and the solutions of the BCS system of two equations; we show Δ_p and Δ_n in the middle and bottom parts of fig. 5.

The next figures presented in this letter are obtained after finding the least action trajectory, as explained previously [21]. We compare in fig. 4 the absolute values of shell and pairing correction energies for symmetrical fission of ^{260}Rf with R_2 constant (dashed line) and linearly increasing R_2 (solid line). While for $R_2 =$ const the two-hump barrier is clearly seen, a completely different shape, with a deep minimum near the nuclear surface, may be seen when R_2 is linearly increasing. As expected, the gap for protons, Δ_p, and neutrons, Δ_n, solutions of the BCS system of two equations, in fig. 5 are also following similar variations. Deep minima around $(R-R_i)/(R_t-R_i) = 0.82$ are seen in both figures.

Similar results are also obtained for the SH nucleus ^{264}Sg (see fig. 5). In this figure we compare the shell plus pairing corrections (top) with the BCS gap for neutrons (solid line) and protons (dashed line) for linearly increasing R_2 (central panel) and the BCS gap for neutrons and protons for $R_2 =$ const (bottom). At the touching point, $R = R_t$, both kinds of variations of $R_2 = R_2(R)$ arrive at

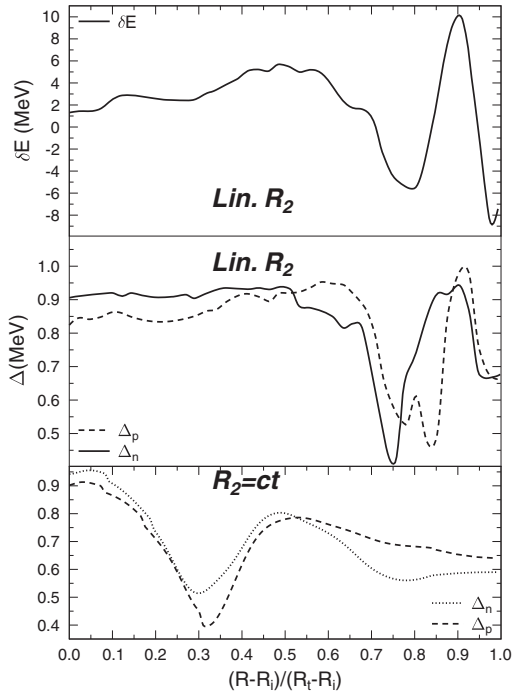

Fig. 5: Comparison of the shell plus pairing corrections (top) with the BCS gap for neutrons (solid line) and protons (dashed line) for linearly increasing R_2 (central panel) and the BCS gap for neutrons and protons for $R_2 =$ const (bottom).

the same state, hence the shell effects are identical there, as may be seen in figs. 4 and 5. We observe in all figures the deep minima near the nuclear surface obtained by using a linearly increasing R_2.

For minimization of action we need not only B_{RR} but also the values of $B_{R_2R_2}, B_{R_2R}$ in every point of the above-mentioned grid. As expected we obtained a dynamical path very different from the statical one.

We could reproduce, with errors lower than one order of magnitude, the experimental values of ^{260}Rf and ^{264}Sg spontaneous fission half-lives, $\log_{10} T_f^{exp}(s) = -1.678$, and -1.432, respectively, by obtaining shorter half-lives: $\log_{10} T_f^{theor}(s) = -1.867$, and -1.511, respectively.

Conclusions. – In conclusion, with our method of calculating the spontaneous fission half-life including the macroscopic-microscopic method for deformation energy based on asymmetric two-center shell model, and the cranking inertia for the dynamical part, we could find a sequence of several trajectories one of which gives the least action. Assuming spherical shapes, we found that the shape parametrization with linearly increasing R_2 is more suitable to describe the fission process of SHs in comparison with that of the exponentially or linearly decreasing law, or $R_2 =$ const. It is in agreement with the microscopic finding for α-decay and cluster radioactivity concerning the preformation of a cluster at the surface, which then penetrates the potential barrier by quantum tunnelling. When $R_2 =$ const one obtains the well-known two-hump shape of the barrier.

The experimental SF half-lives, $\log_{10} T_f^{exp}(s) = -1.678$, and -1.432, respectively, have been well reproduced by minimizing the action integral. Until we perform more calculations for different nuclides we cannot be sure that our positive results are obtained only by chance.

* * *

This work was supported within the IDEI Programme with UEFISCDI, and NUCLEU Programme PN16420101/2016 Bucharest.

REFERENCES

[1] Gamow G., *Z. Phys.*, **51** (1928) 204.
[2] Gurney R. W. and Condon E. U., *Nature*, **122** (1928) 439.
[3] Rose H. J. and Jones G. A., *Nature*, **307** (1984) 245.
[4] *Encyclopaedia Britannica Online*, `http://www.britannica.com/EBchecked/topic/465998/`.
[5] Lovas R. G., Liotta R. J., Insolia A., Varga K. and Delion D. S., *Phys. Rep.*, **294** (1998) 265.
[6] Lane A. M., *Rev. Mod. Phys.*, **32** (1960) 519.
[7] Poenaru D. N., Ivaşcu M. and Mazilu D., *J. Phys. (Paris), Lett.*, **41** (1980) L589.
[8] Wang Y., Wang S., Hou Z. and Gu J., *Phys. Rev. C*, **92** (2015) 064301.
[9] Polikanov S. M., Druin V., Karnaukhov V., Mikheev V., Pleve A., Skobelev N., Subotin V., Ter Akopian G. and Fomichev V., *Sov. Phys. JETP*, **15** (1962) 1016.
[10] Strutinsky V. M., *Nucl. Phys. A*, **95** (1967) 420.
[11] Greiner W. and Poenaru D. N., in *Radioactivity* in *Encyclopedia of Condensed Matter Physics*, edited by Bassani F., Liedl G. L. and Wyder P., Vol. **5** (Elsevier, Oxford) 2005, pp. 106–116.
[12] Hamilton J. H., Hofmann S. and Oganessian Y., *Annu. Rev. Nucl. Part. Sci.*, **63** (2013) 383.
[13] Oganessian Y. T., *Nature*, **413** (2001) 122.
[14] Poenaru D. N., Gherghescu R. A. and Greiner W., *Phys. Rev. Lett.*, **107** (2011) 062503.
[15] Sobiczewski A., *Radiochim. Acta*, **99** (2011) 395.
[16] Staszczak A., Baran A. and Nazarewicz W., *Phys. Rev. C*, **87** (2013) 024320.
[17] Warda M. and Egido J. L., *Phys. Rev. C*, **84** (2011) 044608.
[18] Bjørnholm S., Borggreen J., Echt O., Hansen K., Martin T. P., Pedersen J. and Rasmussen H. D., *Phys. Rev. Lett.*, **65** (1990) 1627.
[19] Poenaru D. N., Gherghescu R. A., Plonski I. H., Solov'yov A. V. and Greiner W., *Eur. Phys. J. D*, **47** (2008) 379.
[20] Knight W. D., Clemenger K., de Heer W. A., Saunders W. A., Chou M. Y. and Cohen M. L., *Phys. Rev. Lett.*, **52** (1984) 2141; **53** (1984) 510.
[21] Poenaru D. N. and Gherghescu R. A., *Phys. Rev. C*, **94** (2016) 014309.
[22] Poenaru D. N. and Gherghescu R. A., *Eur. Phys. J. A*, **52** (2016) 349.
[23] Brack M., Damgaard J., Jensen A., Pauli H. C., Strutinsky V. M. and Wong G. Y., *Rev. Mod. Phys.*, **44** (1972) 320.
[24] Gherghescu R. A., *Phys. Rev. C*, **67** (2003) 014309.
[25] Krappe H. J., Nix J. R. and Sierk A. J., *Phys. Rev. C*, **20** (1979) 992.
[26] Signarbieux C., Montoya M., Ribrag M., Mazur C., Guet C., Perrin P. and Maurel M., *J. Phys. (Paris), Lett.*, **42** (1981) L437.
[27] Baran A., Kowal M., Reinhard P.-G., Robledo L. M., Staszczak A. and Warda M., *Nucl. Phys. A*, **944** (2015) 442.
[28] Warda M. and Robledo L. M., *Phys. Rev. C*, **84** (2011) 044608.
[29] Bardeen J., Cooper L. and Schrieffer J., *Phys. Rev. C*, **108** (1957) 1175.